Research Square

Preprints are preliminary reports that have not undergone peer review.
They should not be considered conclusive, used to inform clinical practice,
or referenced by the media as validated information.

Pharmacological Inhibition of Rab7A Sensitizes Bortezomib-Resistant Multiple Myeloma Cells by Disrupting Lysosomal Adaptation and Stem-Like Features

Guluzar Gulnur Itez

gulnuritez@gmail.com

Ankara University

Tulin Ozkan

Ankara University

Doga Tezal Altindag

Ankara University

Kubra Gayret Aslan

Ankara University

Asuman Sunguroğlu

Ankara University

Meral Beksaç

Istinye University

Research Article

Keywords: Multiple myeloma, bortezomib resistance, lysosomal adaptation, Rab7A, CID1067700, lysosomal stemness

Posted Date: November 18th, 2026

DOI: https://doi.org/10.21203/rs.3.rs-11097077/v1

License: This work is licensed under a Creative Commons Attribution 4.0 International License.
Read Full License

Additional Declarations: No competing interests reported.

Pharmacological Inhibition of Rab7A Sensitizes Bortezomib-Resistant Multiple Myeloma Cells by Disrupting Lysosomal Adaptation and Stem-Like Features

Guluzar Gulnur Itez[1,2] PhD, Tulin Ozkan[1,3] PhD, Doga Tezal Altindag[1,3]MSc, Kubra Gayret Aslan[1,3]MSc, Asuman Sunguroglu[1,2,3] PhD, Meral Beksaç[4] PhD

[1]: Ankara University, Institute of Health Sciences, Ankara, Turkey

[2]: Ankara University, Stem Cell Institute, Ankara, Turkey

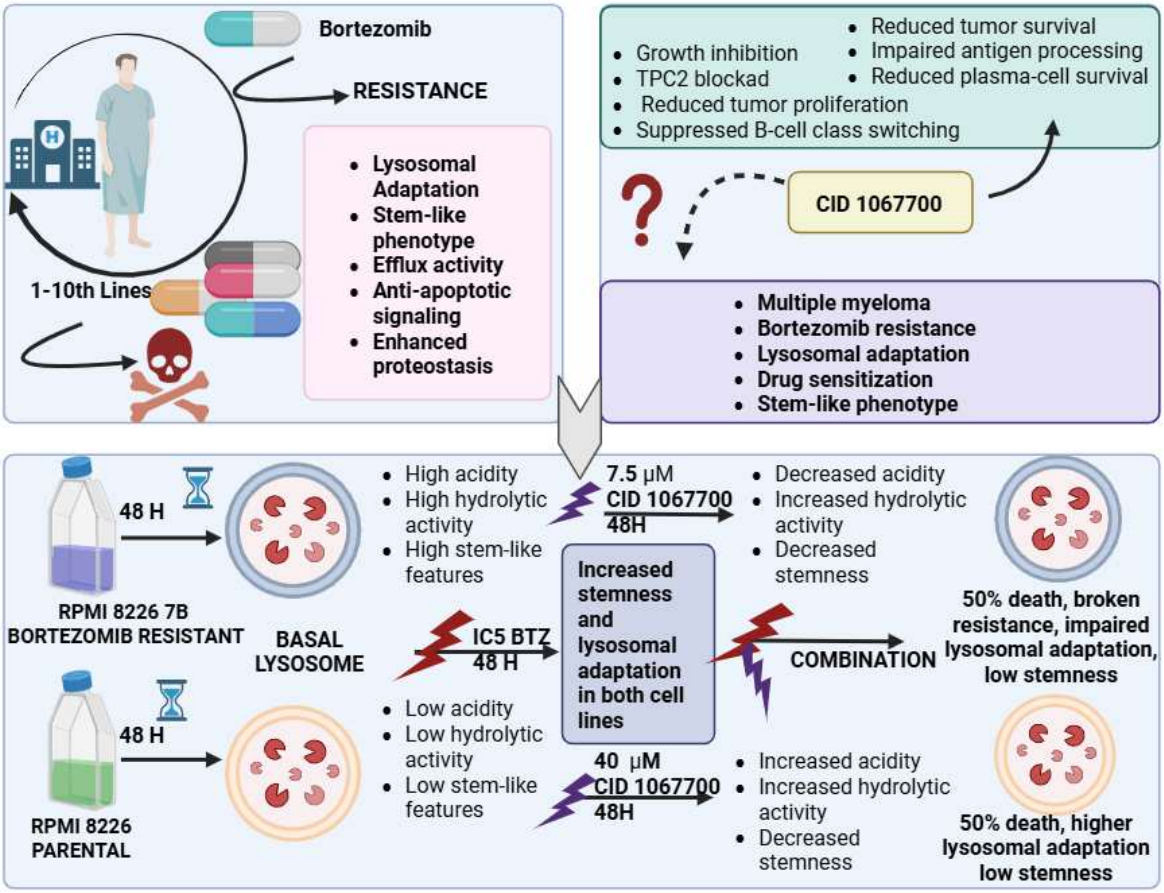
[3]: Ankara University, Faculty of Medicine, Department of Medical Biology, Ankara, Turkey

[4]: Ankara Liv Hospital, Istinye University, Ankara, Turkey

Corresponding author:

Gülüzar Gülnur ITEZ, PhD: Ankara University, Institute of Health Sciences, Ankara, Turkey, E-mail: gulnuritez@gmail.com

Graphical abstract



Abstract

Objective: Bortezomib resistance limits durable responses in multiple myeloma treatment. This study investigated whether pharmacological targeting of Rab7A with CID1067700 could disrupt lysosomal adaptation and resensitize bortezomib-resistant myeloma cells.

Methods: Dose–response profiles of bortezomib and CID1067700 were determined by MTT assay in bortezomib-sensitive RPMI 8226 and resistant RPMI 8226-7B cells. Combination effects were evaluated using Bliss independence and Highest Single Agent models. Lysosomal acidification and hydrolytic activity were assessed by flow cytometry, RAB7A protein levels by ELISA, and related gene expression by qPCR. CID1067700–RAB7A interactions were examined by molecular docking. RAB7A expression was also evaluated in bone marrow samples from patients with newly diagnosed multiple myeloma (NDMM), relapsed/refractory multiple myeloma (RRMM), and healthy controls.

Results: RPMI 8226-7B cells were 5.7-fold more resistant to bortezomib but showed no marked cross-resistance to CID1067700. Low-dose bortezomib increased CID1067700 sensitivity 1.2-fold in parental cells and 7.8-fold in resistant cells, with a maximum Bliss score of 47.93. Resistant cells exhibited higher basal lysosomal acidification and hydrolytic activity. CID1067700 reduced lysosomal acidification by approximately 25.3-fold at 48 h and suppressed the bortezomib-induced increase in hydrolytic activity. The combination increased the BAX/BCL2 ratio, while CID1067700 reduced BCRP/ABCG2, SOX2, OCT4, and NANOG expression in resistant cells. RAB7A expression was higher in RRMM samples.

Conclusion: Pharmacological Rab7 targeting disrupted lysosomal dependence and strongly resensitized bortezomib-resistant myeloma cells. Rab7A-regulated lysosomal homeostasis may represent a targetable vulnerability in bortezomib resistance.

Keywords: Multiple myeloma, bortezomib resistance, lysosomal adaptation, Rab7A, CID1067700, lysosomal stemness

1. Introduction

Multiple myeloma (MM) is a hematological malignancy characterized by the clonal proliferation of terminally differentiated plasma cells in the bone marrow. The high production of immunoglobulins and anti-apoptotic proteins makes myeloma cells dependent on proteostasis mechanisms [1,2]. The introduction of proteasome inhibitors into clinical practice represented a major milestone in MM management, with bortezomib becoming a key component of treatment across different stages of the disease. However, intrinsic or acquired bortezomib resistance continues to limit durable treatment responses [3,4].

Bortezomib suppresses proteasomal protein degradation, leading to the accumulation of misfolded and damaged proteins, proteotoxic stress, and cell death [5,6]. Surviving myeloma cells may activate alternative protein clearance pathways to compensate for proteasome inhibition [7,8]. Among these, the autophagy–lysosome system is a major adaptive survival mechanism for removing accumulated proteins [2,9]. Increased lysosomal acidification, proteolytic activity, and autophagic degradation may support cellular survival under proteasomal stress, and this adaptation may be more prominent in resistant cells with enhanced drug efflux capacity and stem-like properties [10,11]. Although lysosome-targeting agents and

v-ATPase inhibitors have shown preclinical efficacy in combination with proteasome inhibitors, their clinical translation has remained limited [12–14].

Rab7A is a small GTPase that regulates late endosome maturation, endosome–lysosome trafficking, lysosomal positioning, and autophagosome–lysosome fusion [15]. Its role in cancer varies according to cell type and biological context; it has been associated with proliferation, invasion, and disease progression, while tumor-suppressive effects have also been reported [16]. Therefore, Rab7A may be considered a central regulator of endolysosomal organization and cellular adaptation in a context-dependent manner. In cancer, Rab7A has been investigated predominantly through gene silencing, whereas its pharmacological targeting remains limited [17].

CID1067700 is a pan-GTPase inhibitor that suppresses guanine nucleotide binding to Rab7 and thereby limits Rab7-dependent functions [18]. Although it has been used to investigate Rab7 function in various cellular models [19–23], the effects of Rab7 inhibition on lysosomal adaptation and proteostasis in cancer cells remain insufficiently characterized.

In this study, we investigated whether pharmacological inhibition of Rab7A could disrupt lysosomal adaptation and resensitize bortezomib-resistant MM cells. The effects of CID1067700 alone and in combination with low-dose bortezomib were compared in bortezomib-sensitive RPMI 8226 and resistant RPMI 8226-7B cells. Cell viability, lysosomal function, Rab7A, apoptosis, drug resistance, and markers associated with stem-like phenotypes were evaluated. We hypothesized that resistant MM cells would be more dependent on Rab7A-mediated lysosomal homeostasis and therefore exhibit selective sensitivity to Rab7A targeting.

2. Methods

This study was designed to evaluate the effects of pharmacological Rab7 targeting on cell viability, lysosomal function, and related molecular responses in bortezomib-sensitive and -resistant multiple myeloma (MM) cells. Cell line-specific dose–response profiles were established for bortezomib and CID1067700, and IC_5 and IC_{50} values were determined. CID1067700 concentrations producing approximately 50% cytotoxicity in combination with IC_5 bortezomib were identified by combination analyses. Lysosomal hydrolytic activity and acidification, intracellular RAB7A protein levels, and selected gene expression were evaluated in control, bortezomib, CID1067700, and combination groups. The CID1067700–RAB7A interaction was additionally investigated by molecular docking analysis.

2.1. Cell lines and culture conditions

Bortezomib-sensitive RPMI 8226 cells were cultured in L-glutamine-containing RPMI 1640 medium (Sigma-Aldrich, R7509) supplemented with 10% FBS and 1% penicillin/streptomycin (MERCK-SIGMA, P4333-100 mL), whereas resistant RPMI 8226-7B cells were cultured in RPMI 1640 medium supplemented with 1% GlutaMAX™ Supplement (Gibco™) and 1% penicillin/streptomycin. Cells were incubated at 37°C and 5% CO_2 (Nüve EC160-03.0862); the medium was renewed every three days, and the doubling time was determined to be approximately 26 hours. RPMI 8226-7B cells were provided by Dr. Javier Naval (University of Zaragoza) [24]. To maintain the resistance phenotype, cells were treated with 15 nM bortezomib (Merck-Millipore, CAS: 179324-69-7) every three months for one week, followed by a two-week drug-free recovery period. Cells with appropriate viability, morphology, and proliferation characteristics in the logarithmic growth phase were used for experiments.

2.2. Drug treatments and experimental groups

Bortezomib and CID1067700 (Sigma-Aldrich, SML0545-5MG; CAS: 314042-01-8) were stored in DMSO (Merck, 116743.1000). Working solutions were prepared in culture medium and diluted 1:10 in the culture medium to achieve the final concentrations. Cells were divided into control, bortezomib, CID1067700, and bortezomib–CID1067700 combination groups; the control group received an equivalent amount of DMSO. Bortezomib was used at the cell line-specific IC_5 concentration, while CID1067700 was used at the concentration producing approximately 50% cytotoxicity under these conditions. All treatments were performed for 48 hours.

2.3. Cell viability and dose–response analysis

Cell viability was assessed using the MTT assay. RPMI 8226 and RPMI 8226-7B cells were seeded at 5×10^4 cells/mL in 96-well plates and incubated with increasing drug concentrations for 48 hours. MTT reagent (GLPBIO, GC14731-500) was added, and cells were incubated for two hours. The resulting formazan crystals were dissolved in an appropriate solvent, and absorbance was measured using a microplate reader (Epoch, BioTek). After subtraction of solvent background, viability was calculated as a percentage of the control, and IC_5 and IC_{50} values were determined from dose–response curves.

For combination analysis, cells were exposed to cell line-specific IC_5 bortezomib and increasing concentrations of CID1067700 for 48 hours. Combination effects were evaluated using the Bliss independence and Highest Single Agent (HSA) models. Expected Bliss viability (%) = [CID1067700 single-agent viability (%) × bortezomib single-agent viability (%)]/100; Bliss score = expected viability − observed combination viability. HSA expected viability was defined as the lowest viability observed under either single-agent condition, and the HSA score was calculated as HSA expected viability − observed combination viability. Positive, near-zero, and negative scores were interpreted as synergistic, additive, and antagonistic interactions, respectively.

2.4. Flow cytometric assessment of lysosomal functions

Lysosomal hydrolytic activity and acidification were assessed using a BD Accuri™ C6 Flow Cytometer. Staining was performed according to the manufacturers' protocols; an equal number of events was collected from each sample, and results were analyzed based on mean fluorescence intensity (MFI). Hydrolytic activity was measured using the Lysosomal Intracellular Activity Assay Kit (Abcam, ab234622) and expressed as relative activity compared with the control. Lysosomal acidification was assessed using the BioTracker™ NIR633 probe (MERCK-SIGMA, SCT138), with MFI used as an indicator of lysosomal acidification.

2.5. RNA isolation and quantitative real-time PCR

Total RNA was isolated from control and drug-treated groups using RiboEx™ reagent (301-001); RNA quantity and purity were assessed spectrophotometrically. cDNA was synthesized from equal amounts of RNA using the iScript™ cDNA Synthesis Kit (Bio-Rad, 1708890). Gene expression was analyzed by quantitative real-time PCR using SuperFast RT Master Mix for qPCR (GLPBIO, GK10031-250). RAB7A, SOX2, OCT4, NANOG, ABCG2/BCRP, CD24, CD38, CTSB, BAX, and BCL2 were evaluated. Expression levels were normalized to GAPDH and calculated using the 2^−ΔCt method; the BAX/BCL2 ratio was additionally evaluated as a transcriptional indicator of apoptotic tendency.

2.6. Bone marrow samples and ethical approval

The study protocol was approved by the Ankara University Human Research Ethics Committee on June 13, 2024 (Application No.: 2024000387-2; Decision No.: İ06-434-24) and was conducted in accordance with the Declaration of Helsinki and national ethical regulations. Written informed consent was obtained from all participants. Two milliliters of bone marrow aspirate were homogenized with 1 mL RiboEx and stored at −80°C; RNA isolation, quantification, and cDNA synthesis were performed using the same methods as for cell samples. RAB7A expression was analyzed in NDMM (n = 22), RRMM (n = 34), and healthy control (n = 4) samples using the 2^−ΔCt method. Detailed clinical data were not included because they were outside the scope of the ethical and institutional approvals.

2.7. Determination of intracellular RAB7A protein levels

Following drug treatment, cells were lysed by five freeze–thaw cycles in PBS. Total protein levels were determined using the BCA method (Takara, T9300A), and samples were normalized to equal protein amounts. RAB7A levels were measured using a human RAB7A-specific ELISA kit (BT-Lab, E6785Hu) according to the manufacturer's protocol. Concentrations were calculated from a standard curve and normalized to total protein.

2.8. Molecular docking analysis

Blind molecular docking analysis was performed to assess the potential interaction between CID1067700 and human RAB7A. The three-dimensional model of human RAB7A, AF-P51149-F1, was used; the SMILES structures of CID1067700 and the natural ligand GTP were prepared as ligands, and the protein surface was screened for potential binding sites. The most favorable binding poses of CID1067700, predicted binding energies, and interacting amino acid residues were analyzed, and two- and three-dimensional interaction maps were generated.

2.9. Statistical analysis and data visualization

Data were obtained from at least three independent biological experiments and presented as mean ± standard deviation. One-way ANOVA was used for single-factor comparisons, while two-way ANOVA followed by Tukey's multiple-comparison test was used for analyses involving both cell line and treatment. For heatmap visualization, group means for each gene were converted to z-scores [$z = (x - \mu)/\sigma$], where x represents the 2^−ΔCt value, μ the group mean, and σ the standard deviation. Z-scores were used only for visualization, whereas statistical analyses were performed using 2^−ΔCt values.

3. Results

3.1. Bortezomib resistance and sensitivity to CID1067700 as a single agent

3.1.1. RPMI 8226-7B cells exhibit increased resistance to bortezomib

Bortezomib induced dose-dependent loss of viability in both cell lines; however, RPMI 8226-7B cells were more resistant. Bortezomib IC_{50} values were 7.07 ± 0.55 and 40.22 ± 1.83 nM in RPMI 8226 and RPMI 8226-7B cells, respectively, representing an approximately 5.7-fold higher value in resistant cells. CID1067700 IC_{50} values were 50.40 ± 3.40 and 58.52 ± 2.64 μM, respectively. The similar sensitivity to CID1067700 indicated that bortezomib resistance did not confer marked cross-resistance (Figure 1).

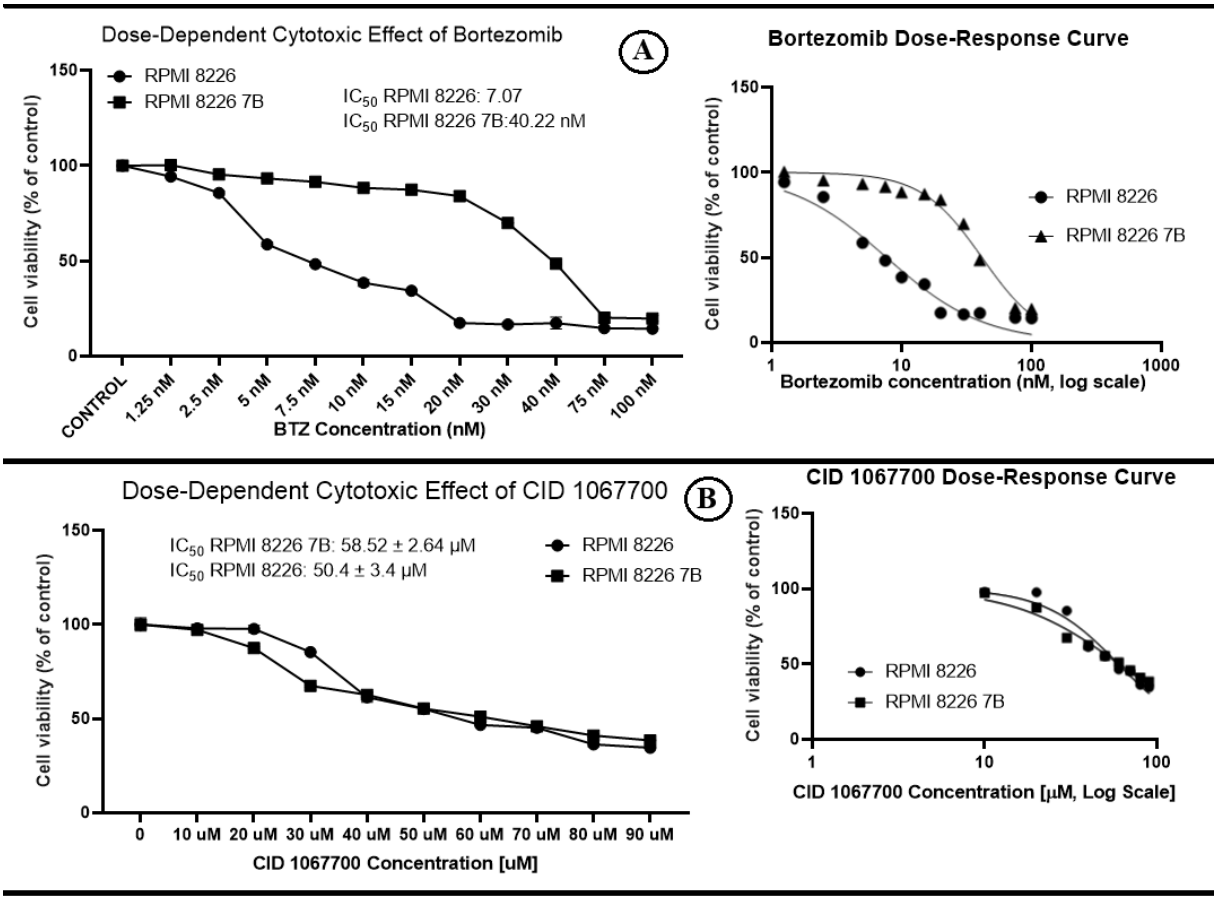


Figure 1. Cell viability was assessed by MTT assay following 48 h treatment with bortezomib or CID1067700. (A) Bortezomib IC_{50} values were 7.07 ± 0.55 and 40.22 ± 1.83 nM in RPMI 8226 and RPMI 8226-7B cells, respectively; (B) CID1067700 IC_{50} values were 50.40 ± 3.40 and 58.52 ± 2.64 μM, respectively. Data are presented as mean ± standard deviation from three independent biological experiments, each performed with three technical replicates.

3.2. Low-dose bortezomib markedly increases the sensitivity of RPMI 8226-7B cells to CID1067700

In the presence of low-dose bortezomib, the CID1067700 IC_{50} decreased from 50.40 ± 3.40 μM to 41 μM in RPMI 8226 cells and from 58.52 ± 2.64 μM to 7.5 μM in RPMI 8226-7B cells, corresponding to 1.2- and 7.8-fold increases in sensitivity, respectively. In resistant cells, the

combination of 5 nM bortezomib and 7.5 µM CID1067700 reduced viability to approximately 50%. Bliss scores were positive across a broader concentration range in resistant cells, with the highest score of 47.93 observed for the combination of 20 µM CID1067700 and 5 nM bortezomib (Figure 2).

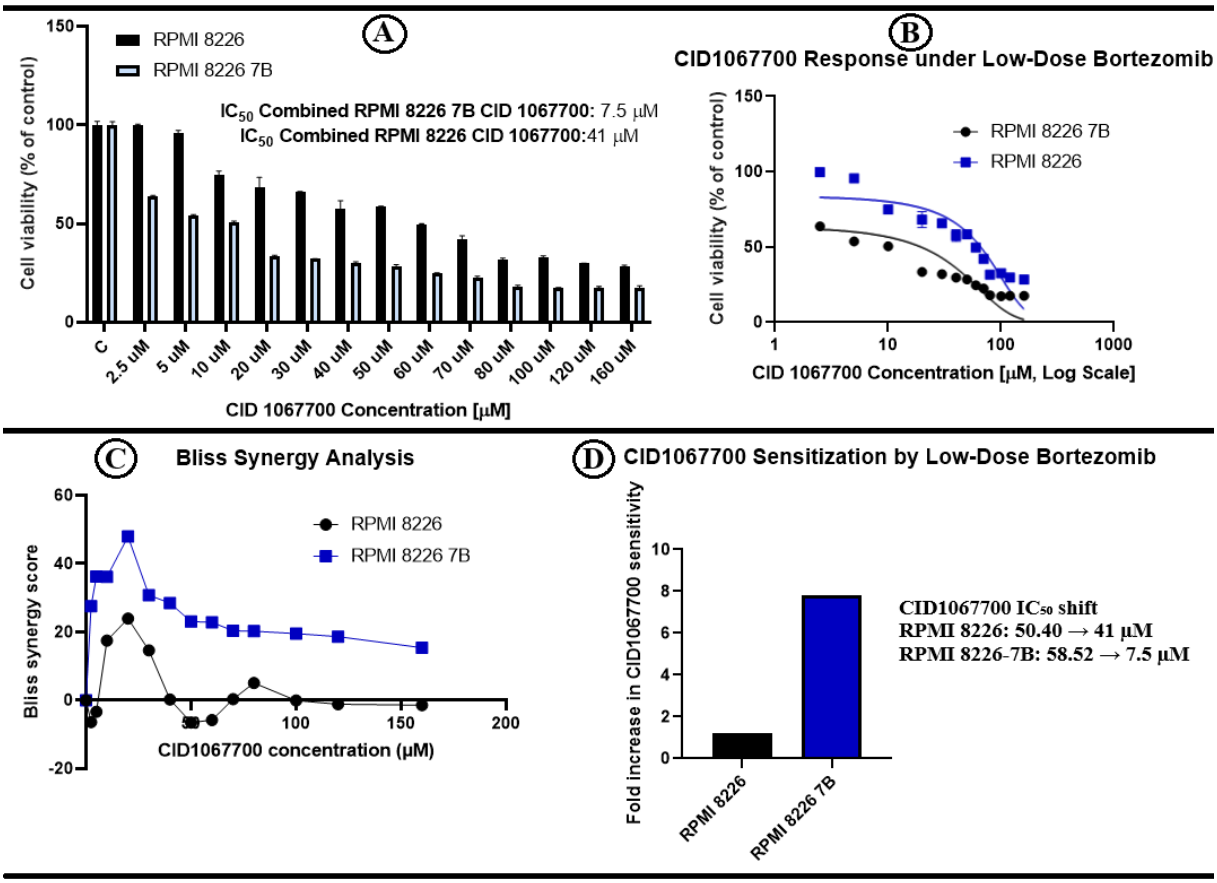


Figure 2. Effect of low-dose bortezomib on CID1067700 sensitivity RPMI 8226 and RPMI 8226-7B cells were incubated for 48 h with increasing concentrations of CID1067700 in the presence of 1.25 and 5 nM bortezomib, respectively. (A) Cell viability following combination treatment. (B) Combination dose–response curves and CID1067700 IC_{50} values. (C) Bliss synergy scores. (D) Increase in sensitivity calculated from single-agent and combination IC_{50} values. Data are presented as mean ± standard deviation from three independent biological experiments.

3.3. RAB7A expression and molecular findings associated with CID1067700

RAB7A expression was higher in RRMM samples (0.715614 ± 0.838631) than in NDMM (0.231406 ± 0.182157) and healthy controls (0.010972 ± 0.01448). Although basal RAB7A mRNA levels appeared higher in RPMI 8226-7B cells, the difference was not significant. Bortezomib increased RAB7A expression in resistant cells ($p < 0.001$), whereas CID1067700 decreased it, with the combination bringing expression closer to control levels ($p < 0.001$). In parental cells, RAB7A expression remained above control levels following CID1067700 treatment ($p = 0.0167$). At the protein level, the combination was associated with lower RAB7A

levels than either single-agent treatment in both cell lines. Docking analysis indicated that CID1067700 could occupy a nucleotide-binding groove overlapping with that of GTP. The predicted binding pose showed contacts with D16, S17, G18, V19, G20, K21, and T22 in the P-loop region; N125, K126, D128, L129, and K157 in the guanine-recognition region; and G34, N35, Q36, Y37, and K38 at the Switch I/II boundary. These findings support the possibility that CID1067700 occupies the nucleotide-binding pocket of RAB7A.

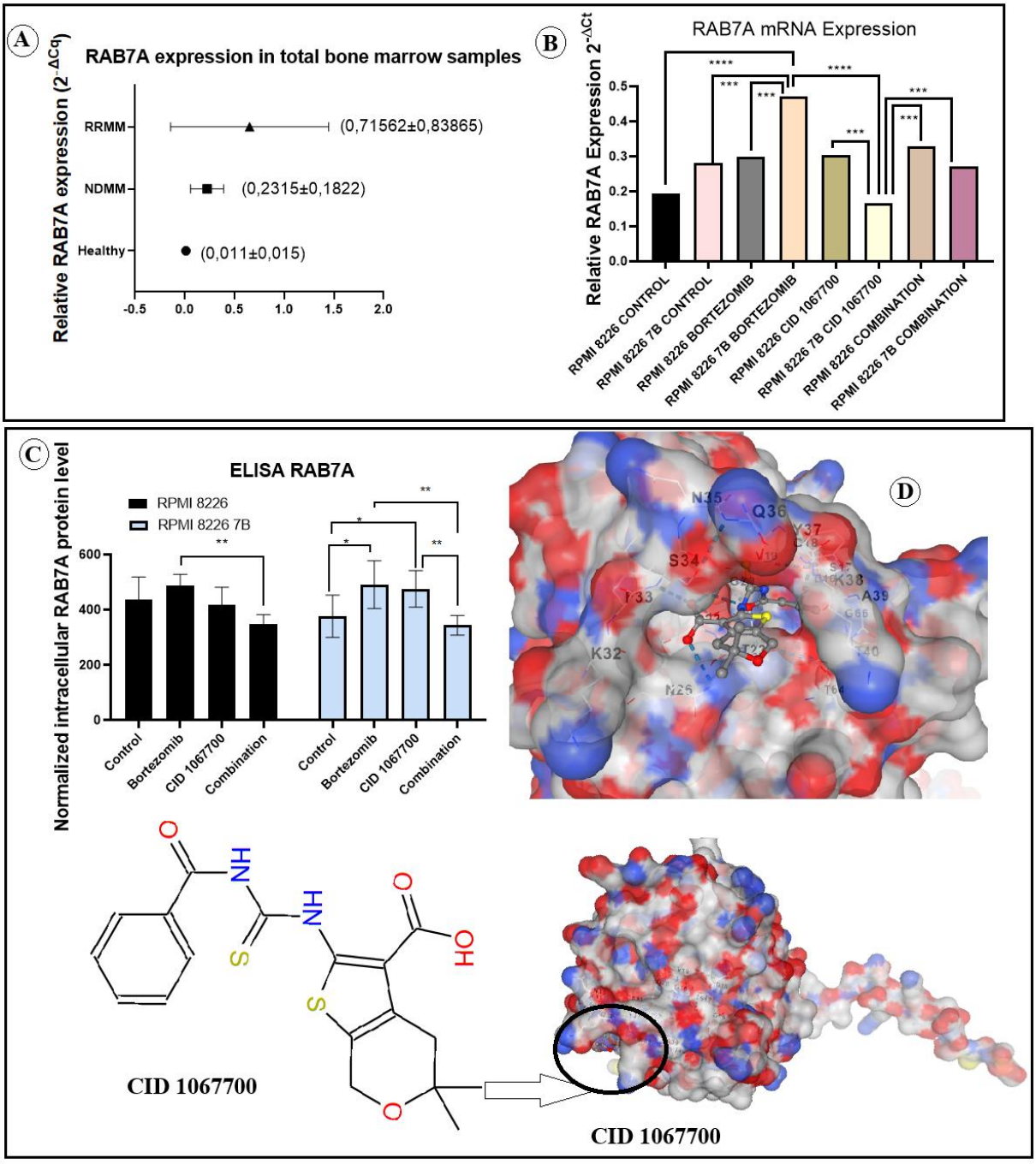


Figure 3. RAB7A expression in clinical samples and cell line models and the predicted binding mode of CID1067700. (A) RAB7A expression in total bone marrow samples from healthy controls, patients with newly diagnosed multiple myeloma, and patients with relapsed/refractory multiple myeloma. (B) Effects of bortezomib,

CID1067700, and combination treatment on RAB7A mRNA expression in RPMI 8226 and RPMI 8226-7B cells. (C) Intracellular RAB7A protein levels normalized to total protein. Cell line data are presented as mean ± standard deviation from three independent biological experiments. (D) Formulation of CID1067700, its predicted positioning within the nucleotide-binding region of RAB7A, and close-up views of the binding pocket.

3.4. CID1067700 increased the stress response in resistant cells, reduced BCRP/ABCG2 expression, and enhanced apoptotic tendency with combination treatment

BCRP/ABCG2 expression increased following bortezomib treatment in resistant cells but decreased with CID1067700. In parental cells, the opposite response was observed, with CID1067700 increasing BCRP/ABCG2 expression. In resistant cells, combination treatment resulted in lower expression than bortezomib alone but higher expression than CID1067700 alone.

BAX and BCL2 mRNA expression levels were assessed separately, and the BAX/BCL2 ratio was calculated to evaluate apoptotic tendency. In RPMI 8226-7B cells, low-dose bortezomib increased both BAX and BCL2 expression, whereas both remained close to control levels following low-dose CID1067700. In parental RPMI 8226 cells, CID1067700 significantly reduced BCL2 expression compared with controls ($p = 0.00021$). Combination treatment increased the BAX/BCL2 ratio above 1 in both cell lines, indicating a shift toward an apoptotic response. BCRP/ABCG2 expression responses varied according to cell line and treatment condition.

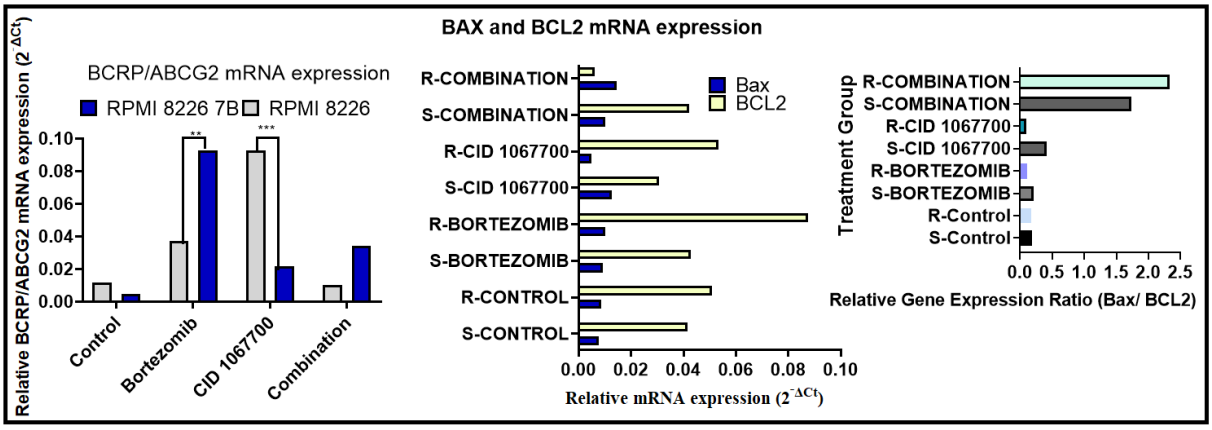


Figure 4. Effects of CID1067700 and bortezomib on gene expression related to proteostasis, drug resistance, and apoptotic tendency. BAX and BCL2 mRNA expression, BAX/BCL2 ratio, and BCRP/ABCG2 mRNA expression were assessed by qPCR in bortezomib-sensitive RPMI 8226 cells (S, sensitive) and bortezomib-resistant RPMI 8226-7B cells (R, resistant) following 48 h of control, bortezomib, CID1067700, or combination treatment. Gene expression was calculated using the $2^{-}\Delta Ct$ method. BAX and BCL2 expression levels are presented separately, and the BAX/BCL2 ratio was calculated to assess apoptotic tendency. Statistical significance is indicated on the graphs: *$p < 0.05$, **$p < 0.01$, ***$p < 0.001$, and ****$p < 0.0001$.

3.5. CID1067700 rapidly and strongly reduced lysosomal acidification in resistant cells

Basal lysosomal acidification was higher in RPMI 8226-7B cells than in parental cells ($p < 0.0001$). Bortezomib increased acidification in both cell lines, with a more pronounced increase in resistant cells. In contrast, CID1067700 markedly reduced lysosomal acidity, particularly in RPMI 8226-7B cells. In the time-course analysis, the 48-h control MFI in resistant cells decreased from 8787 to 330 following CID1067700 treatment, corresponding to a 25.3-fold reduction, whereas the change in parental cells was limited (0.441-fold).

3.5.1. CID1067700 reduced bortezomib-induced lysosomal hydrolytic activity

Basal lysosomal hydrolytic activity was higher in RPMI 8226-7B cells. CID1067700 at the single-agent IC_{50} reduced activity in both cell lines, with a greater effect in resistant cells. In the low-dose combination setting, 7.5 μM CID1067700 reduced hydrolytic activity in resistant cells, whereas 41 μM CID1067700 produced a more limited effect in parental cells. Bortezomib increased hydrolytic activity, particularly in resistant cells, whereas combination treatment reduced this increase.

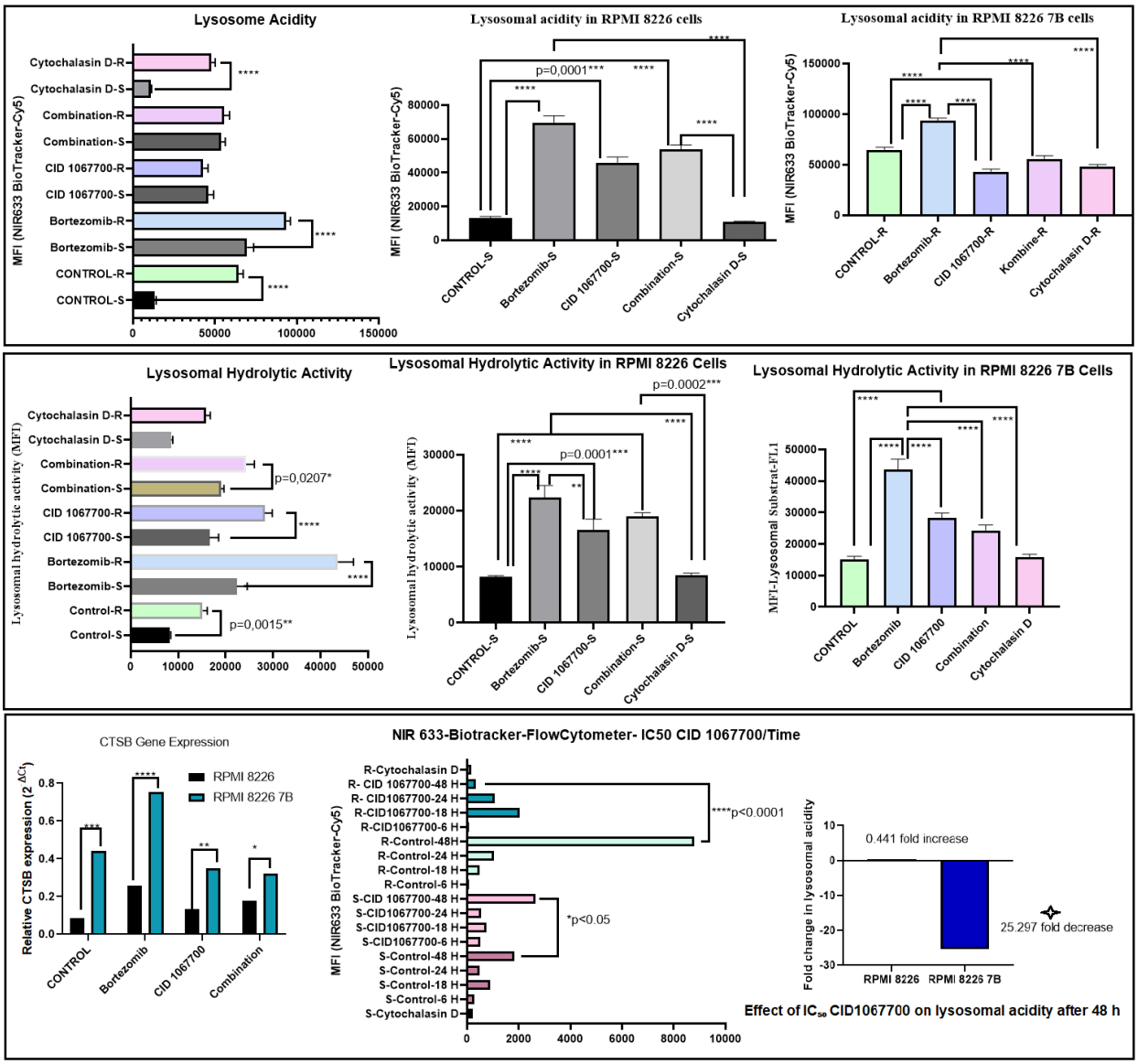


Figure 5. Effects of CID1067700 on lysosomal acidity and hydrolytic activity in bortezomib-sensitive and -resistant multiple myeloma cells. Lysosomal acidity was assessed using the NIR633 BioTracker-Cy5 fluorescent probe, and lysosomal hydrolytic activity using a fluorescent lysosomal substrate by flow cytometry. RPMI 8226 sensitive cells (S, sensitive) and bortezomib-resistant RPMI 8226-7B cells (R, resistant) were incubated for 48 h under control, bortezomib, CID1067700, or bortezomib–CID1067700 combination conditions. Cytochalasin D was used as a positive control. Comparisons between cell lines and treatment groups were based on MFI values. CTSB mRNA expression was measured by qPCR and presented as relative expression using the $2^{-}\Delta Ct$ method. The time-dependent effect of CID1067700 on lysosomal acidity was assessed after 6, 18, 24, and 48 h. At 48 h, CID1067700 increased lysosomal acidity 0.441-fold in RPMI 8226 cells and reduced it 25.297-fold in RPMI 8226-7B cells. Statistical significance is indicated on the graphs: *p < 0.05, **p < 0.01, ***p < 0.001, and ****p < 0.0001.

3.6. CID1067700 reduced expression of stemness-associated markers, particularly in bortezomib-resistant cells

Bortezomib increased SOX2, OCT4, NANOG, and CD24 expression, particularly in RPMI 8226-7B cells, whereas CID1067700 markedly reduced these markers. SOX2 and NANOG

expression reached their lowest levels in the combination group. OCT4 showed higher basal expression in resistant cells but decreased to similar levels in both cell lines following CID1067700 treatment and was further reduced in resistant cells by combination treatment. CD24 increased with bortezomib but fell below control levels with CID1067700; combination treatment reduced its expression compared with bortezomib alone but remained above control levels. CD38 increased with CID1067700 in sensitive cells, whereas it was further reduced by CID1067700 and combination treatment in resistant cells. The heatmap showed an overall suppression of stemness-associated transcripts following CID1067700 and combination treatment.

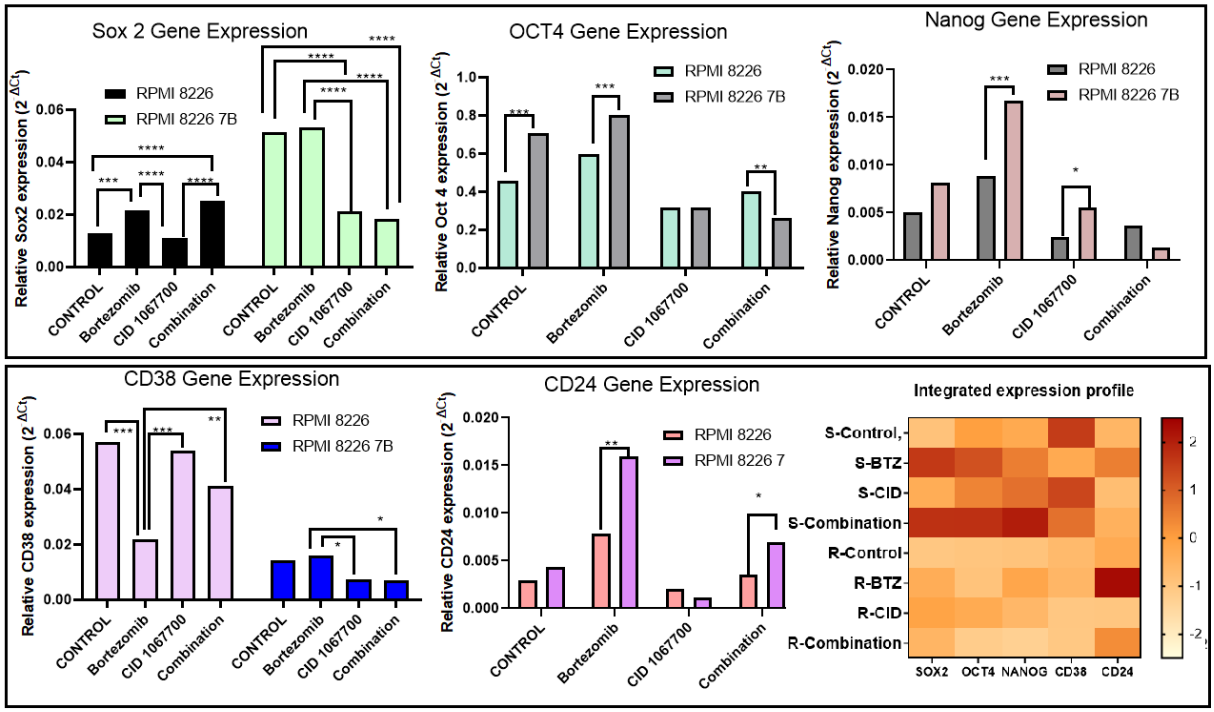


Figure 6. Effects of CID1067700 and bortezomib on gene expression associated with the stemness phenotype. SOX2, OCT4, NANOG, CD38, and CD24 mRNA expression was assessed by qPCR in RPMI 8226 and bortezomib-resistant RPMI 8226-7B cells following 48 h of control, bortezomib, CID1067700, or combination treatment. Gene expression was normalized to GAPDH and calculated using the $2^{-}\Delta Ct$ method. The heatmap shows integrated expression patterns after conversion of group means for each gene to z-scores. Statistical significance is indicated on the graphs: *p < 0.05, **p < 0.01, ***p < 0.001, and ****p < 0.0001.

4. Discussion

This study demonstrates that pharmacological Rab7 targeting with CID1067700 disrupts lysosomal adaptation in bortezomib-resistant multiple myeloma (MM) cells and markedly increases their sensitivity to low-dose bortezomib. Although RPMI 8226-7B cells were approximately 5.7-fold more resistant to bortezomib than parental RPMI 8226 cells, they did not show significant cross-resistance to CID1067700 [24]. More importantly, in the presence of low-dose bortezomib, the CID1067700 IC_{50} decreased from 58.52 to 7.5 μM in resistant

cells, corresponding to a 7.8-fold increase in sensitivity, compared with only 1.2-fold in parental cells. The broader concentration range with positive Bliss scores and a maximum score of 47.93 in resistant cells further support the hypothesis that CID1067700 may overcome bortezomib resistance.

Bortezomib resistance is associated not only with direct alterations in the proteasome but also with alternative mechanisms for managing proteotoxic burden. Cells surviving proteasome inhibition may become increasingly dependent on the autophagy–lysosome system to remove accumulated and misfolded proteins. Higher basal lysosomal acidification and hydrolytic activity in RPMI 8226-7B cells indicate an enhanced lysosomal capacity. The further increase in both parameters following bortezomib, particularly in resistant cells, is consistent with adaptive activation of the lysosomal system under proteasomal stress [7–9]. Thus, lysosomes represent not a passive compartment but a functional component of resistance that contributes to maintenance of proteostatic integrity during bortezomib treatment.

One of the most prominent effects of CID1067700 was the rapid and strong suppression of lysosomal acidification in resistant cells. In RPMI 8226-7B cells, the MFI decreased from 8787 to 330 at 48 h, corresponding to an approximately 25.3-fold reduction, whereas no marked suppression was observed in parental cells. CID1067700 also reduced the bortezomib-induced increase in hydrolytic activity. The simultaneous impairment of acidification and hydrolytic activity suggests that CID1067700 affects lysosomal function required to maintain proteolytic capacity in resistant cells. Thus, while bortezomib increases proteotoxic burden, CID1067700 may limit its lysosomal compensation, contributing to the strong cytotoxic effect of the combination.

Higher CTSB expression in resistant cells and its further increase following bortezomib are also consistent with enhanced lysosomal proteolytic capacity [9]. However, CTSB mRNA levels are not necessarily expected to parallel lysosomal hydrolytic activity under all conditions, as lysosomal function is also determined by compartmental acidity, enzyme maturation, membrane trafficking, and lysosomal positioning [25]. Therefore, the strong effect of CID1067700 on acidification may functionally limit overall hydrolytic capacity even without complete suppression of lysosomal gene expression. This finding highlights the importance of flow cytometric functional measurements as complementary parameters to transcriptional analyses.

The RAB7A findings indicate a complex, treatment-dependent response to pharmacological targeting. Higher RAB7A expression in RRMM bone marrow samples than in NDMM and healthy controls suggests that the RAB7A axis may be more prominent in advanced or treatment-resistant disease. However, this comparison should be considered exploratory, particularly because of the small healthy control group and the lack of detailed clinical data within the available permissions. In cell models, the increase in RAB7A mRNA following bortezomib in resistant cells may reflect increased proteostatic capacity, whereas suppression of this increase by CID1067700 may indicate failure to induce pathways supporting Rab7 activation. Further pathway analyses are warranted in future studies.

RAB7A protein levels did not consistently parallel the mRNA findings. This discrepancy may be related to post-transcriptional regulation, as Rab7A expression has been reported to be regulated by several miRNAs [26]. In particular, the increase in RAB7A protein in resistant cells after CID1067700 despite reduced mRNA expression may reflect a compensatory response to functional Rab7 inhibition or weak activation of gene expression associated with impaired late endosome/lysosome activity. Conversely, the lower RAB7A protein levels observed in combination groups may be associated with increased apoptotic tendency and overall cellular stress. However, these interpretations were not directly demonstrated; assessment of protein synthesis, protein turnover, and the GTP-bound active Rab7A pool is required. Thus, the present findings suggest that CID1067700 may disrupt Rab7-dependent functions rather than simply altering RAB7A expression.

Molecular docking results further supported the potential targeting of the RAB7A nucleotide-binding region by CID1067700. The predicted binding pose overlapped with residues in the P-loop, guanine recognition region, and Switch I/II boundary, consistent with a potential limitation of GTP binding and associated conformational transitions [18,27]. However, because CID1067700 is a pan-GTPase inhibitor, these findings should not be interpreted as demonstrating absolute Rab7A specificity. Genetic Rab7A suppression or rescue experiments are required to determine the extent to which the observed pharmacological effects are Rab7A-dependent.

In resistant cells, BCRP/ABCG2 expression increased following bortezomib but decreased with CID1067700. This finding suggests that CID1067700 may weaken a component of the resistance phenotype associated with drug efflux by suppressing BCRP/ABCG2 expression.

However, direct efflux/influx activity analyses are required to determine the effect of CID1067700 on drug transport [4].

The increase in the BAX/BCL2 ratio above 1 following combination treatment in both cell lines indicates that loss of viability was accompanied by pro-apoptotic transcriptional changes. However, BAX and BCL2 mRNA levels alone do not establish apoptosis. Therefore, these findings should be interpreted as indicating that the combination may increase cellular susceptibility to the intrinsic apoptotic response; functional analyses including caspase activation, Annexin V/PI staining, mitochondrial membrane potential, and PARP cleavage could further validate this mechanism [29].

Cellular plasticity associated with bortezomib resistance may also be linked to stem cell-like properties. In our study, bortezomib increased SOX2, OCT4, NANOG, and CD24 expression, particularly in RPMI 8226-7B cells, whereas CID1067700 suppressed most of these markers. The lowest NANOG expression in both cell lines following combination treatment, together with marked suppression of SOX2 and OCT4 in resistant cells, suggests that lysosomal targeting may also affect resistance-associated cellular states. The overall transcriptional suppression observed in the heatmap supports this interpretation [4].

Although a previous study reported that bortezomib effectively targets side population cells in RPMI 8226 cells, changes in SOX2, OCT4, and NANOG after treatment were not assessed [30]. Therefore, the ability of bortezomib to eliminate side population cells does not demonstrate suppression of the stemness program in surviving cells. In our study, the increase in stemness markers following bortezomib, particularly in resistant cells, suggests that stem cell-like properties may be enhanced in cells surviving treatment.

The CD38 findings require a more cautious interpretation. Although CD38 is a classical marker of mature plasma cell differentiation, some studies have also associated it with stem cell-like or aggressive phenotypes [31]. In our study, CD38 levels were lower in resistant cells and further decreased with CID1067700, despite suppression of SOX2, OCT4, and NANOG, indicating that CD38 is a context-dependent marker. Therefore, stemness in MM should be evaluated using integrated transcriptional and phenotypic patterns rather than a single surface marker.

Taken together, our findings support a model in which resistant RPMI 8226-7B cells possess higher basal lysosomal capacity, further increase this capacity under bortezomib treatment, and consequently become more susceptible to pharmacological Rab7 targeting. Although CID1067700 showed similar single-agent IC_{50} values in both cell lines, low-dose bortezomib produced strong sensitization only in resistant cells. This suggests that CID1067700 acts less as a conventional selective cytotoxic agent and more by targeting the lysosomal dependence that emerges under bortezomib treatment. In other words, while bortezomib increases proteotoxic burden, CID1067700 limits its lysosomal compensation and thereby removes the adaptive advantage of resistant cells.

This study has several limitations. The experiments were limited to two related cell lines, requiring validation in MM models with different genetic backgrounds. The absence of treatment regimen, line of therapy, autologous stem cell transplantation, and other clinical variables in patient samples precluded assessment of the relationship between RAB7A expression and clinical characteristics. The small healthy control group also limits interpretation of patient data. Furthermore, because CID1067700 is a pan-GTPase inhibitor, not all observed effects can be attributed directly to Rab7A inhibition. Many gene expression findings were not validated at the protein or functional level, and the therapeutic efficacy of the combination was not evaluated in vivo.

Nevertheless, this study characterizes the effects of pharmacological Rab7 targeting in the context of bortezomib resistance by integrating lysosomal function, proteostatic responses, drug sensitization, and stem cell-like features. To our knowledge, this is the first study to demonstrate the effects of CID1067700 in MM cells, particularly its impact on lysosomal acidification and hydrolytic activity in the context of bortezomib resistance. These findings suggest that Rab7-regulated lysosomal homeostasis represents a targetable adaptive vulnerability in bortezomib-resistant myeloma cells and may provide a basis for evaluating this axis as a strategy for resensitization to proteasome inhibitors.

References

[1] S.V. Rajkumar, Multiple myeloma: 2024 update on diagnosis, risk-stratification, and management, American J Hematol 99 (2024) 1802–1824. https://doi.org/10.1002/ajh.27422.

[2] O.S. Al-Odat, D.A. Guirguis, N.K. Schmalbach, G. Yao, T. Budak-Alpdogan, S.C. Jonnalagadda, M.K. Pandey, Autophagy and Apoptosis: Current Challenges of Treatment and Drug Resistance in Multiple Myeloma, Int J Mol Sci 24 (2022) 644. https://doi.org/10.3390/ijms24010644.

[3] S. Ito, Proteasome Inhibitors for the Treatment of Multiple Myeloma, Cancers 12 (2020) 265. https://doi.org/10.3390/cancers12020265.

[4] G. Kozalak, İ. Bütün, E. Toyran, A. Koşar, Review on Bortezomib Resistance in Multiple Myeloma and Potential Role of Emerging Technologies, Pharmaceuticals (Basel) 16 (2023) 111. https://doi.org/10.3390/ph16010111.

[5] M. Ri, Endoplasmic-reticulum stress pathway-associated mechanisms of action of proteasome inhibitors in multiple myeloma, Int J Hematol 104 (2016) 273–280. https://doi.org/10.1007/s12185-016-2016-0.

[6] M. Takenokuchi, K. Miyamoto, K. Saigo, T. Taniguchi, Bortezomib Causes ER Stress-related Death of Acute Promyelocytic Leukemia Cells Through Excessive Accumulation of PML-RARA, Anticancer Res 35 (2015) 3307–3316.

[7] A.M. Elshazly, N. Hosseini, J. Vangala, S. Shen, V. Neely, X. Hu, P.P. Pagare, H. Harada, S. Grant, S.K. Radhakrishnan, Proteasome Inhibition Enhances Lysosome-mediated Targeted Protein Degradation, (2025). https://doi.org/10.1101/2025.01.31.634950.

[8] C. Alecki, J. Rizwan, P. Le, S. Jacob-Tomas, M.F. Comaduran, M. Verbrugghe, J.M.S. Xu, S. Minotti, J. Lynch, J. Biswas, T. Wu, H.D. Durham, G.W. Yeo, M. Vera, Localized molecular chaperone synthesis maintains neuronal dendrite proteostasis, Nat Commun 15 (2024) 10796. https://doi.org/10.1038/s41467-024-55055-7.

[9] R. Zhang, X. Yang, X. Shi, E. Xing, L. Wang, C. Hao, Z. Zhang, Bortezomib modulated the autophagy-lysosomal pathway in a TFEB-dependent manner in multiple myeloma, Leukemia Research 138 (2024) 107455. https://doi.org/10.1016/j.leukres.2024.107455.

[10] R. Franqui-Machin, E.B. Wendlandt, S. Janz, F. Zhan, G. Tricot, Cancer stem cells are the cause of drug resistance in multiple myeloma: fact or fiction?, Oncotarget 6 (2015) 40496–40506. https://doi.org/10.18632/oncotarget.5800.

[11] J. Abdi, G. Chen, H. Chang, Drug resistance in multiple myeloma: latest findings and new concepts on molecular mechanisms, Oncotarget 4 (2013) 2186–2207. https://doi.org/10.18632/oncotarget.1497.

[12] P. Robak, I. Drozdz, J. Szemraj, T. Robak, Drug resistance in multiple myeloma, Cancer Treatment Reviews 70 (2018) 199–208. https://doi.org/10.1016/j.ctrv.2018.09.001.

[13] V. Pinto, R. Bergantim, H.R. Caires, H. Seca, J.E. Guimarães, M.H. Vasconcelos, Multiple Myeloma: Available Therapies and Causes of Drug Resistance, Cancers 12 (2020) 407. https://doi.org/10.3390/cancers12020407.

[14] S. Meister, B. Frey, V.R. Lang, U.S. Gaipl, G. Schett, U. Schlötzer-Schrehardt, R.E. Voll, Calcium Channel Blocker Verapamil Enhances Reticulum Stress and Death Induced by Proteasome Inhibition in Myeloma Cells, Neoplasia 12 (2010) 550-IN3. https://doi.org/10.1593/neo.10228.

[15] M. Cabrera, C. Ungermann, Guiding Endosomal Maturation, Cell 141 (2010) 404–406. https://doi.org/10.1016/j.cell.2010.04.013.

[16] F. Guerra, C. Bucci, Multiple Roles of the Small GTPase Rab7, Cells 5 (2016) 34. https://doi.org/10.3390/cells5030034.

[17] J. Xie, Y. Yan, F. Liu, H. Kang, F. Xu, W. Xiao, H. Wang, Y. Wang, Knockdown of Rab7a suppresses the proliferation, migration, and xenograft tumor growth of breast cancer cells, Bioscience Reports 39 (2019) BSR20180480. https://doi.org/10.1042/BSR20180480.

[18] J.O. Agola, L. Hong, Z. Surviladze, O. Ursu, A. Waller, J.J. Strouse, D.S. Simpson, C.E. Schroeder, T.I. Oprea, J.E. Golden, J. Aubé, T. Buranda, L.A. Sklar, A. Wandinger-Ness, A Competitive Nucleotide Binding Inhibitor: *In Vitro* Characterization of Rab7 GTPase Inhibition, ACS Chem. Biol. 7 (2012) 1095–1108. https://doi.org/10.1021/cb3001099.

[19] L. Hong, P. Simons, A. Waller, J. Strouse, Z. Surviladze, O. Ursu, C. Bologa, K. Gouveia, J.O. Agola, S. BasuRay, A. Wandinger-Ness, L. Sklar, D.S. Simpson, C.E. Schroeder, J.E. Golden, J. Aubé, A small molecule pan-inhibitor of Ras-superfamily GTPases with high efficacy towards Rab7, in: Probe Reports from the NIH Molecular Libraries Program, National Center for Biotechnology Information (US), Bethesda (MD), 2010. http://www.ncbi.nlm.nih.gov/books/NBK143553/ (accessed May 24, 2026).

[20] M. Fernandez, R. Wang, J. Wang, S. Wu, K. Holder, A. Nazarullah, R.C.T. Aguiar, Z.Y. Xu-Monette, K.H. Young, H. Yan, Z. Xu, Targeting RAB7 in human B lymphoma by a small molecule inhibitor arrests tumor cell growth, Front. Oncol. 15 (2025) 1616519. https://doi.org/10.3389/fonc.2025.1616519.

[21] T. Lam, D.V. Kulp, R. Wang, Z. Lou, J. Taylor, C.E. Rivera, H. Yan, Q. Zhang, Z. Wang, H. Zan, D.N. Ivanov, G. Zhong, P. Casali, Z. Xu, Small Molecule Inhibition of Rab7 Impairs B Cell Class Switching and Plasma Cell Survival To Dampen the Autoantibody Response in Murine Lupus, The Journal of Immunology 197 (2016) 3792–3805. https://doi.org/10.4049/jimmunol.1601427.

[22] C. Abrahamian, R. Tang, R. Deutsch, L. Ouologuem, E.-M. Weiden, V. Kudrina, J. Blenninger, J. Rilling, C. Feldmann, S. Kuss, Y. Stepanov, A.S. Rosato, G.T. Calvo, M.S. Soengas, D. Mayr, T. Fröhlich, T. Gudermann, M. Biel, C. Wahl-Schott, C.-C. Chen, K. Bartel, C. Grimm, Rab7a is an enhancer of TPC2 activity regulating melanoma progression through modulation of the GSK3β/β-Catenin/MITF-axis, Nat Commun 15 (2024) 10008. https://doi.org/10.1038/s41467-024-54324-9.

[23] M. Runsala, E. Kuokkanen, E. Uski, V. Šuštar, M.Ö. Balci, J. Rajala, V. Paavola, P.K. Mattila, The Small GTPase Rab7 Regulates Antigen Processing in B Cells in a Possible Interplay with Autophagy Machinery, Cells 12 (2023) 2566. https://doi.org/10.3390/cells12212566.

[24] P. Balsas, N. López-Royuela, P. Galán-Malo, A. Anel, I. Marzo, J. Naval, Cooperation between Apo2L/TRAIL and bortezomib in multiple myeloma apoptosis, Biochemical Pharmacology 77 (2009) 804–812. https://doi.org/10.1016/j.bcp.2008.11.024.

[25] L.K.K. Holland, I.Ø. Nielsen, K. Maeda, M. Jäättelä, SnapShot: Lysosomal Functions, Cell 181 (2020) 748-748.e1. https://doi.org/10.1016/j.cell.2020.03.043.

[26] A.E. Güleç Taşkıran, H.H. Hüsnügil, Z.E. Soltani, G. Oral, N.S. Menemenli, C. Hampel, K. Huebner, K. Erlenbach-Wuensch, I. Sheraj, R. Schneider-Stock, A. Akyol, N. Liv, S. Banerjee, Post-Transcriptional Regulation of Rab7a in Lysosomal Positioning and Drug Resistance in Nutrient-Limited Cancer Cells, Traffic 25 (2024) e12956. https://doi.org/10.1111/tra.12956.

[27] X. Li, D. Li, D. Tang, X. Huang, H. Bao, J. Wang, S. Qi, Cryo-EM structure of the human MON1A−CCZ1−RAB7A complex provides insights into nucleotide exchange mechanism, Life Metabolism 4 (2025) loaf017. https://doi.org/10.1093/lifemeta/loaf017.

[28] F. He, X. Ru, T. Wen, NRF2, a Transcription Factor for Stress Response and Beyond, Int J Mol Sci 21 (2020) 4777. https://doi.org/10.3390/ijms21134777.

[29] M. Mustafa, R. Ahmad, I.Q. Tantry, W. Ahmad, S. Siddiqui, M. Alam, K. Abbas, Moinuddin, Md.I. Hassan, S. Habib, S. Islam, Apoptosis: A Comprehensive Overview of Signaling Pathways, Morphological Changes, and Physiological Significance and Therapeutic Implications, Cells 13 (2024) 1838. https://doi.org/10.3390/cells13221838.

[30] K.H. Kim, H.-J. Cheong, M.Y. Lee, N. Lee, K.-T. Lee, S.K. Park, J.-H. Won, Bortezomib Is More Effective to Side Population of RPMI8226 Myeloma Cells than Classical Anti-myeloma Agents, Anticancer Res 39 (2019) 127–133. https://doi.org/10.21873/anticanres.13088.

[31] M.R. Dyer, A. Zheleznyak, E.N. Teubner, J.L. Prior, B. Manion, Z. Jing, A.K. Sharma, J. Du, R. Tang, M.A. Fiala, J.F. DiPersio, D. Veis, J. O'Neal, M.Y. Berezin, M. Shokeen, Ablation of CD38 in multiple myeloma cells leads to an aggressive phenotype in a mouse xenograft model, Blood Advances 10 (2026) 343–355. https://doi.org/10.1182/bloodadvances.2025017296.

Supplementary Files

This is a list of supplementary files associated with this preprint. Click to download.

- graphicalabstract.png